Atmospheric Research 278 (2022) 106309

Contents lists available at ScienceDirect

Atmospheric Research

journal homepage: www.elsevier.com/locate/atmosres

Long-term trends of ozone and precursors from 2013 to 2020 in a megacity (Chengdu), China: Evidence of changing emissions and chemistry

Yurun Wang [a,b], Xianyu Yang [a,*], Kai Wu [c], Han Mei [d], Isabelle De Smedt [e], Shigong Wang [a], Jin Fan [a], Shihua Lyu [a], Cheng He [f]

[a] Plateau Atmosphere and Environment Key Laboratory of Sichuan Province, School of Atmospheric Sciences, Chengdu University of Information Technology, Chengdu, China
[b] Department of Land, Air, and Water Resources, University of California Davis, Davis, USA
[c] Department of Civil and Environmental Engineering, University of California Irvine, Irvine, USA
[d] Division of Environment and Sustainability, Hong Kong University of Science and Technology, Hong Kong, China
[e] Royal Belgian Institute for Space Aeronomy (BIRA-IASB), Brussels, Belgium
[f] School of Atmospheric Sciences, Sun Yat-sen University, Zhuhai, China

ARTICLE INFO

Keywords:
Ozone
Emission inventory
OMI
TROPOMI
Meteorological variability

ABSTRACT

Elevated ozone (O_3) pollution in the warm season is an emerging environmental concern affecting global highly urbanized megacities. In southwestern China, full characterization of causes for O_3 pollution has been stymied by limited observations and the dominant factors that influence O_3 variability on a long-term basis still lack understanding. Herein, we identified O_3 variations and inferred trends in precursor emissions in Chengdu over 2013–2020 based on extensive ambient measurements, emission inventory, and satellite data. Numerical models were used to investigate the changes in meteorological variability and biogenic emissions. Trends of O_3 in urban areas show deterioration (+14.0% yr^{-1}) between 2013 and 2016 followed by a slight decrease over 2017–2020, while O_3 levels in rural areas generally show a downward trend (−2.9% yr^{-1}) during 2014–2020. Both emission inventory (−3.7% yr^{-1}) and OMI satellite columns (−4.5% yr^{-1}) depict strong decline trends in NO_x emissions, while satellite HCHO columns exhibit a flattened downward trend of VOC emissions (−1.8% yr^{-1}), which caused rural areas shifted from VOCs-limited to transitional or NO_x-limited regime since 2016. Considering metropolitan Chengdu remains VOCs-limited regime over time, the existing regulatory framework involving simultaneous NO_x and VOCs control would result in evident O_3 improvements in the near future. Despite benefits from anthropogenic emission reductions, we demonstrate that meteorological conditions and enhanced biogenic emissions over the warm season could partially or even fully offset effects attributed to emission changes, making the net effects obscure. This finding provides robust evidence of reductions in NO_x and VOCs emission and informs effective O_3 mitigation policies for megacities which undergo similar emission pathways in Chengdu.

1. Introduction

Ground-level ozone (O_3) is a criteria air pollutant formed through photochemical reactions of precursors including volatile organic compounds (VOCs) and nitrogen oxides ($NO_x = NO + NO_2$) in the presence of sunlight (Trainer et al., 2000). As a pollutant with strong oxidizing properties, elevated O_3 levels are detrimental to human health, biodiversity, and ecosystems (Liu et al., 2018; Wang et al., 2020). Exposure to high levels of ambient O_3 caused over 0.25 million premature deaths and 4.1 million disability-adjusted life years (DALYs) globally per year (Cohen et al., 2017), and the global mortality burden attributed to tropospheric O_3 is projected to continuously increase under the changing climate (Orru et al., 2013; Stowell et al., 2017; Westervelt et al., 2019). Although the anthropogenic emissions of NO_x have been reduced substantially attributed to strict emission control strategies (Air Pollution Prevention and Control Action Plan, APPCAP) implemented by the Chinese government since 2013, the major city clusters in China including the North China Plain (NCP) (Lyu et al., 2019), Yangtze River Delta (YRD) (Gao et al., 2017; Zhan and Xie, 2022), Pearl River Delta (PRD) (He et al., 2019) and Sichuan Basin (SCB) (Yang et al., 2020) still frequently suffer from excessive regional O_3 episodes, which has become a prominent threat to public health (Liu and Wang, 2020a, 2020b).

* Corresponding author.
E-mail address: xyang@cuit.edu.cn (X. Yang).

https://doi.org/10.1016/j.atmosres.2022.106309
Received 3 April 2022; Received in revised form 8 June 2022; Accepted 14 June 2022
Available online 20 June 2022

The Sichuan Basin (SCB) is a region situated in southwest China. Owing to the intense anthropogenic activities and frequent stagnant conditions in combination with the complex basin landscape, elevated O_3 levels have been frequently observed throughout the SCB from 2013 to 2020 (Wu et al., 2022). As the capital city of Sichuan Province, Chengdu is a highly urbanized megacity with vehicle ownership over 5 million and 20.9 million residents at the end of 2020 (Fig. S1). The fossil-fuel-dependent industrial infrastructure and strong traffic mobility within the 14,335 km^2 Chengdu city emit substantial primary air pollutants (NO_x, VOCs, primary particle matter (PM), etc.), posing enormous challenges to air quality management and calling for more aggressive mitigation efforts (Zhou et al., 2019). In addition to anthropogenic emissions, strong biogenic VOC (BVOC) emissions emitted from urban green spaces and densely forested surrounding rural areas also contribute to the elevated O_3 levels over Chengdu (Wu et al., 2020; Ma et al., 2022). Epidemiologic studies reported that the probability of exposure to excessive O_3 pollution is even above 70% for the residents of Chengdu (Meng et al., 2021). There remains an urgent need for identifying the governing factors which contribute to the elevated O_3 levels to design effective O_3 control strategy over Chengdu.

Prior studies have examined the variations of O_3 levels and the formation mechanism of O_3 episodes over Chengdu based on ambient measurements and chemical transport models. In field studies, Wu et al. (2017) pointed out the deteriorated O_3 pollution in Chengdu from 2014 to 2016. Tan et al. (2018) utilized an observation-based box model (OBM) to investigate the O_3-VOC-NO_x sensitivity, and reported that alkenes contribute over 50% of the O_3 production in Chengdu. Deng et al. (2019) found that elevated alkenes and aromatics emissions at night are the dominant reasons for O_3 episodes over Chengdu. In terms of numerical modeling, Yang et al. (2020) used the Weather Research and Forecasting and Community Multiscale Air Quality (WRF-CMAQ) model to probe the causes of elevated O_3 concentrations in Chengdu and identified two typical O_3 episodes with dominant effects of regional transport and local emissions, respectively. By using the WRF-CMAQ model coupled with the Integrated Source Apportionment Method (ISAM) module, Yang et al. (2021a) demonstrated that transportation and industrial sectors were governing contributors to O_3 formation in Chengdu, accounting for over 60% of the maximum daily 8 h average (MDA8) O_3 concentration during spring O_3 episodes. Existing studies have identified the roles of elevated anthropogenic emissions and typical meteorological conditions on O_3 levels over Chengdu. However, these studies were mainly focused on examining the changes of O_3 levels in a short period or typical O_3 episodes while the long-term trend remains elusive. Furthermore, the dominant factors that influence the O_3 variability on a long-term basis are still lack of understanding, which crucially limits our ability to deploy systematic O_3 controls in Chengdu.

In this study, we investigate the long-term trends (2013−2020) of O_3 levels across Chengdu and infer the precursor emissions by satellite data derived from OMI and TROPOMI, as well as anthropogenic emission inventory. Furthermore, the WRF and the Model for Emissions of Gases and Aerosols from Nature (MEGAN) model are then adopted to probe the impacts of meteorology and BVOC emissions on O_3 air quality in Chengdu over 2013–2020. In Section 2, the details of ambient measurements, emission inventories, satellite retrievals, and model configurations are presented. The features of emission changes and meteorological variabilities, as well as their effects on O_3-VOCs-NO_x sensitivity and O_3 levels are discussed in Section 3.

2. Methodology

2.1. Air quality and meteorological observations

Hourly observations of air pollutants over Chengdu were collected from the China National Environmental Monitoring Center (CNEMC, http://www.cnemc.cn/) (Locations are shown in Fig. 1c). There are 5 urban stations (JQLH, DSXL, JPJ, SHP and SWY), 2 traffic stations (LJX

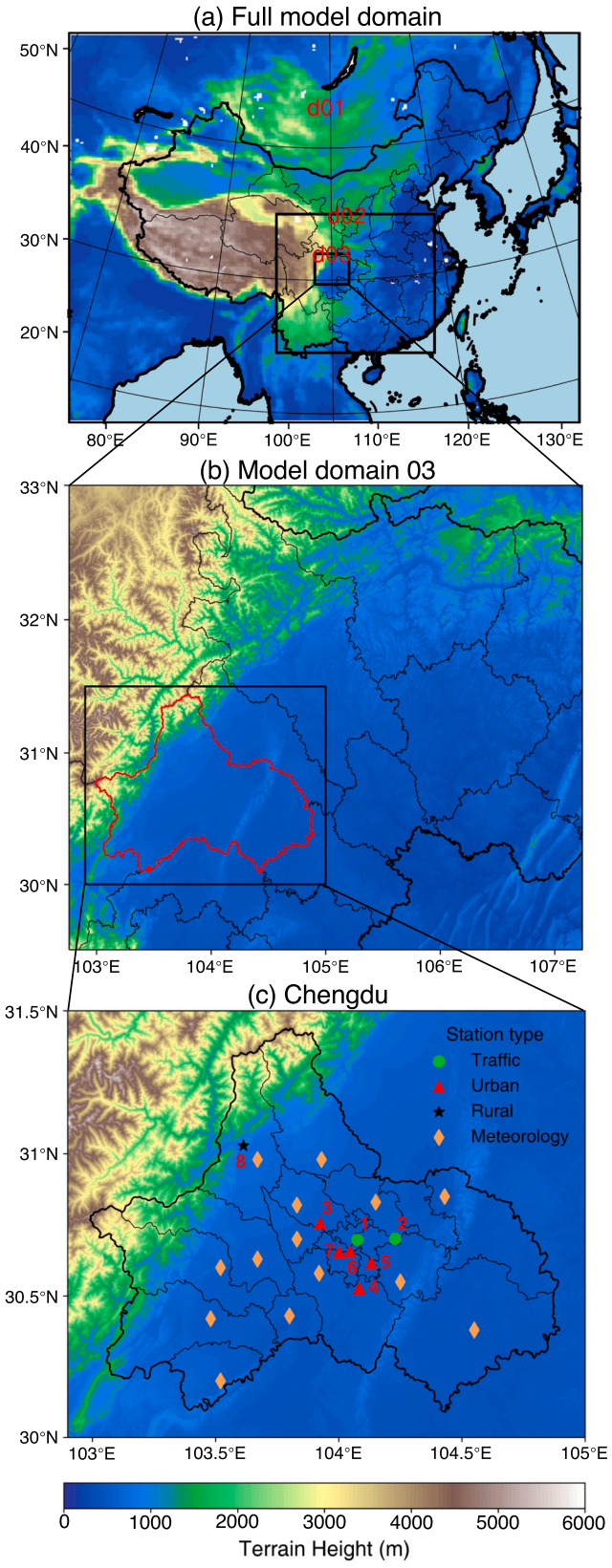

Fig. 1. (a) Map of three nested WRF model domains, (b) the innermost domain and (c) locations of the traffic (green circle), urban (red triangle), rural sites (black pentagram), and meteorological stations (yellow rhombus) over Chengdu. (For interpretation of the references to colour in this figure legend, the reader is referred to the web version of this article.)

and SLD), and 1 rural station (LYS) throughout the Chengdu city. A detailed description of these monitoring sites is presented in Fig. S2 and Table S1. It should be noted that the O_3 measurements are reported in the unit of μg m^{-3} at the standard atmospheric conditions (273.15 K, 1 atm) before September 2018, and at 298.15 K conditions afterwards (MEE, 2012, 2018). To ensure the units of O_3 levels are consistent during 2013–2020, the O_3 concentrations after September 2018 were converted to the standard atmospheric condition.

Surface meteorological observations in Chengdu are provided by the China Meteorological Data Service Center (CMDSC, http://data.cma.cn/) and Sichuan Provincial Weather Service with rigorous data accuracy checks. The hourly data of meteorological parameters including 2-m temperature (T2), 2-m relative humidity (RH2), 10-m wind speed (WS10), and 10-m wind direction (WD10) are used to evaluate the model performance of WRF.

2.2. ERA5 reanalysis

The ERA5 is the fifth generation European Centre for Medium-Range Weather Forecasts (ECMWF) reanalysis with a resolution of 0.25 ° × 0.25 ° (Urraca et al., 2018), which has been widely used for investigating meteorological processes in SCB due to its accurate representation of meteorological parameters (Chen et al., 2021; Yang et al., 2021b).

2.3. Anthropogenic emission inventory

The Multi-resolution Emission Inventory of China (MEIC, http://meicmodel.org/) is a bottom-up emission model developed by Tsinghua University that tracks the variability of anthropogenic emissions in China (Li et al., 2017; Zheng et al., 2018, 2021). The anthropogenic sources were aggregated into five sectors including agriculture, industry, transportation, residential, and power with a spatial resolution of 0.25 ° × 0.25 °. Here, the MEIC emission inventory from 2013 to 2020 was used to probe the long-term changes of anthropogenic NO_x and VOC emissions over Chengdu.

2.4. NO_2 and HCHO columns

To explicitly investigate the trends of NO_x and VOCs emissions over Chengdu, we further adopt the OMI NO_2 and HCHO columns generated by the European Quality Assurance for Essential Climate Variables project (QA4ECV, http://www.qa4ecv.eu/) to characterize spatial changes of NO_x and VOCs (Boersma et al., 2018). The OMI instrument on aboard the NASA's EOS Aura spacecraft measures backscattered solar radiation from the earth in the spectral range 270–500 nm, with a spatial resolution of 13 × 24 km^2 and a bandwidth of 2600 km. OMI provides daily global measurements of NO_2 and HCHO columns with good performance in inferring the trend of NO_x and VOC emissions (De Smedt et al., 2021; Shah et al., 2020; Shen et al., 2019). In addition, the ratio of HCHO and NO_2 columns (FNR) reflects the relative availability of NO_x and VOCs to peroxy radicals, which has been widely used as a metric of regional O_3-VOCs-NO_x sensitivity (Duncan et al., 2010).

The Tropospheric Monitoring Instrument (TROPOMI) instrument is onboard Copernicus Sentinel-5 Precursor platform and was launched in October 2017. The satellite has a sun-synchronous orbit with a daily crossing time at around 13:30 local solar time. The TROPOMI tropospheric NO_2 columns are retrieved with a resolution of 3.5 × 5.5 km in nadir (7 × 5.5 km before August 2019) with algorithms based on the OMI QA4ECV heritage (De Smedt et al., 2018; van Geffen et al., 2020). In addition, TROPOMI Level 2 NO_2 columns are oversampled to 0.01° × 0.01° based on the algorithm developed by Sun et al. (2018), with cloud fraction lower than 30% and quality assurance value higher than 0.75.

2.5. WRF and MEGAN model configurations

Meteorological fields are simulated using the Weather Research and Forecasting (WRFv3.9.1) model. Fig. 1 shows the three nested model domain with horizontal resolutions of 27, 9, 3 km, respectively. The innermost domain covers the Chengdu Plain. There are 30 vertical layers from the ground to 100 hPa, with a surface layer depth of nearly 20 m. The initial and boundary conditions for meteorological fields were obtained from the National Centers for Environmental Prediction (NCEP) Final (FNL) reanalysis data with a resolution of 1.0 ° × 1.0 °. To minimize the influence of initial conditions and cumulative error of the model, the simulations were initialized monthly, treating the 3 days before that month as spin-up. The physical parameterization schemes selected in the WRF model are listed in Table S2. The evaluation of WRF model performance is presented in Text S1 and Table S3.

MEGANv2.1 was driven by meteorological fields from WRF model to estimate the BVOC emissions for the innermost domain (Guenther et al., 2012). Plant function types (PFTs) are adopted from the MODIS MCD12Q1 product and emission factors are obtained from global database based on PFT-specific emission factors tabulated in MEGAN. The leaf area index (LAI) is derived from Moderate Resolution Imaging Spectroradiometer (MODIS) MOD15A2H LAI product (Wu et al., 2020). It should be noted that urban LAI is not considered in this work due to the limitation of MODIS LAI products.

2.6. Definition of heat wave and air stagnation

Heat waves (HWs) refer to extremely hot periods that last for several consecutive days, which could lead to severe O_3 episodes by enhancing photochemical reactions and BVOC emissions (Zhao et al., 2019). In this study, the HWs is defined as a period of at least 3 consecutive days with the daily maximum temperature > 34 °C (Huang et al., 2021; Wang et al., 2021).

Air stagnation is characterized by meteorological conditions that impede the scavenging of air pollutants (Xie et al., 2021; Wang et al., 2022). Here, the air stagnation index (ASI) defined by Horton et al. (2012) is used as an indicator of stagnant conditions. A grid cell is considered stagnant on a given day if three conditions are simultaneously met: the daily average wind speed at 10 m < 3.2 m/s, the wind speed at 500 hPa < 13 m/s, and daily total precipitation < 1.0 mm.

3. Results and discussion

3.1. NO_2 and O_3 trends over Chengdu during 2013–2020

Fig. 2 presents the April–September averaged MDA8 O_3 and daytime NO_2 concentrations (09:00–18:00 LST) across Chengdu during 2013–2020 around a map of TROPOMI tropospheric NO_2 columns with ambient measurements in 2020. Spatially, both satellite NO_2 columns and ambient measurements observed elevated NO_2 levels (30.1 μg/m^3) over metropolitan area of Chengdu due to intense anthropogenic emissions, while NO_2 concentrations are comparatively low (11.2 μg/m^3) at the rural site. More pronounced negative trends in NO_2 levels (−2.8 μg m^{-3} yr^{-1}) are detected at traffic stations than monitors in urban (−1.6 μg m^{-3} yr^{-1}) and rural (−1.2 μg m^{-3} yr^{-1}) areas over the period. It is important to note that average daytime NO_2 concentrations at traffic sites are even lower than at urban sites since 2018 (Fig. 3a), which provides direct evidence of regulations efforts on reducing traffic NO_x emissions over time.

Unlike continuous decreases in NO_2 levels, O_3 levels exhibit strong inter-annual variability given the non-linear dependence on precursor emissions. For urban and traffic sites, deteriorated trend (+14.0% yr^{-1}) of average MDA8 O_3 is observed during 2013–2016 and O_3 levels endure weak reductions with notable interannual variability afterwards. In particular, O_3 concentration descended by −14.1% from 2016 to 2017 and increased by 6.8% during 2019–2020. In contrast, O_3 concentrations at the rural site generally show a downward trend (−2.9% yr^{-1}) during 2014–2020. The reasons for these inconsistent O_3 trends between metropolitan and rural areas could be related to the combined effects of emission changes and different O_3-VOC-NO_x sensitivity (discussed

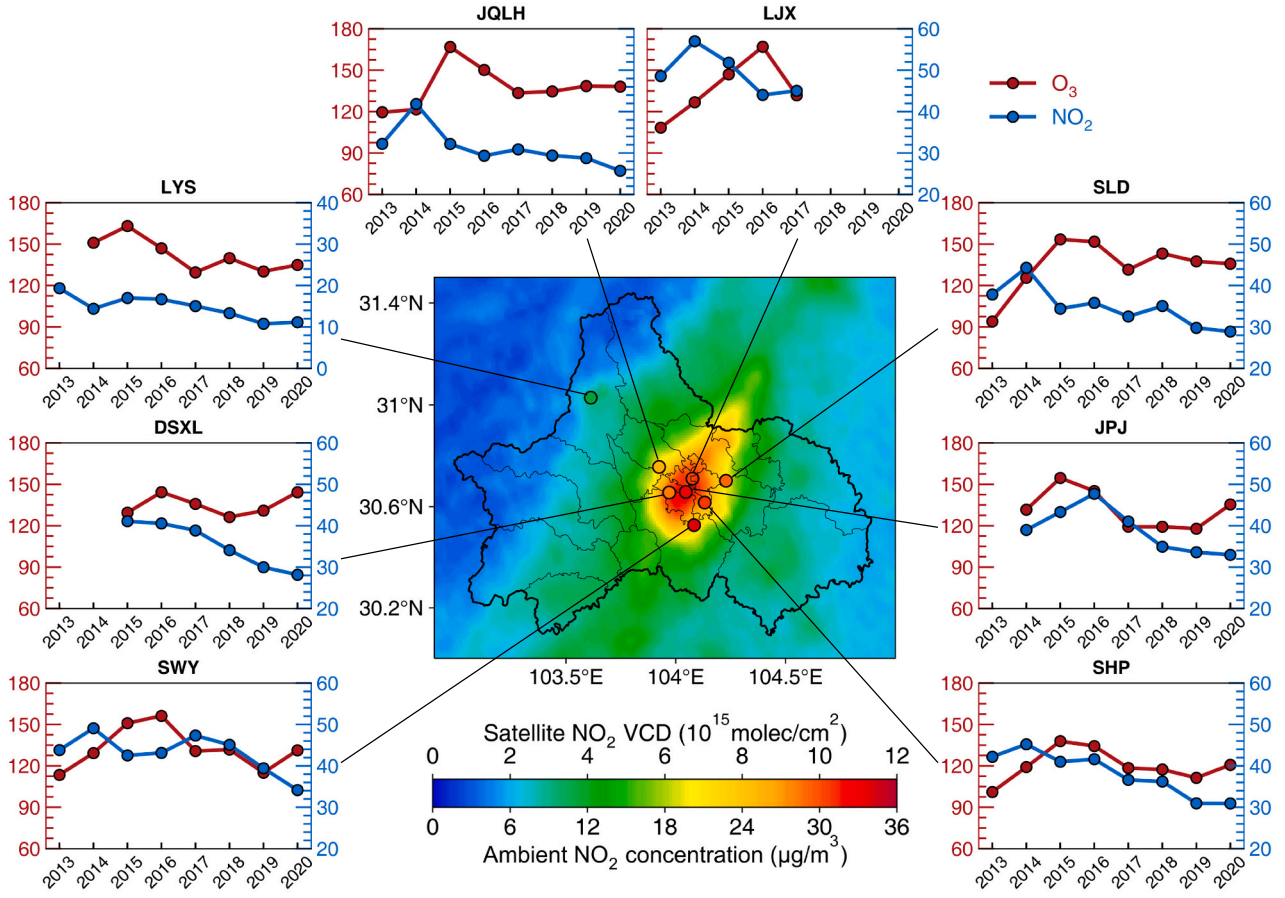

Fig. 2. (Middle panel) TROPOMI NO_2 column densities overlaid with averaged (April–September) ambient measured daytime NO_2 concentrations for 2020 in Chengdu. Time series of averaged (April–September) daytime NO_2 and MDA8 O_3 in μg/m^3 for each site over April–September in Chengdu from 2013 to 2020.

later). It is worth noting that O_3 level at the rural station is comparable or even higher than urban and traffic stations in the spring season, reflecting the effects of regional transport and contribution from background O_3. Furthermore, the monthly average MDA8 O_3 concentrations generally show bimodal distribution for the months between April and September, with peaks in May (Fig. 3b). This pattern could be linked to the O_3 subsidence from the upper troposphere governed by synoptic-scale force, which has been reported in Liu et al. (2019) and Yang et al. (2021a). Following Kalabokas et al. (2017), the specific humidity anomaly and vertical wind speed at 850 hPa from the ERA5 dataset were used as an indicator of the tropospheric subsidence. Fig. S3 illustrates the occurrence frequencies of positive omega vertical velocity accompanied by negative specific humidity anomalies in May are significantly higher than in other months over the SCB, suggesting that strong subsidence from the upper troposphere could contribute to the elevated O_3 levels in May over Chengdu.

3.2. Trends of anthropogenic NO_x and VOC emissions over Chengdu

To further explore the variations of NO_x and VOC emissions in Chengdu, the sectoral trends of anthropogenic NO_x and VOC emissions from MEIC during 2013–2020 are presented in Fig. 4. In addition, emission changes of NO_x and VOCs attributed to each anthropogenic sector are shown in Fig. 5. For NO_x emissions, the MEIC inventory indicates a remarkable decreasing pattern from 283.2 to 206.5 kt, with a reduction ratio of −3.9% yr^{-1} during 2013–2020, which is slightly higher than the reduction rate (−3.7% yr^{-1}) over the SCB (Wu et al., 2022). This significant decreasing trend is in line with the national emission controls (APPCAP: standard GB 13223–2011) since 2013 (Zheng et al., 2018). Furthermore, the government of Chengdu has further developed the local strategies to combat air pollution, and put great emphasis on controlling the emission of motor vehicles (Fig. 5) (Gao et al., 2020). Therefore, the contribution of transportation sector decreases from 48.4% to 45.2% during 2013–2019, and industrial sector has been the largest contributor to NO_x emissions since 2015. However, a sharp drop in industrial NO_x emissions was found in 2020 (Fig. 6a) due to the substantial suspend of industrial activities during the Covid-19 pandemic (Zheng et al., 2021), which leads to the contribution of transportation sector rebounded to 48.0% in 2020.

For anthropogenic VOC emissions, the trend shows a fluctuation pattern with a slight increase from 404.8 to 419.3 kt in 2014 and remains at high levels during 2014–2017. Since August 2017, a stringent VOC emissions standard (DB51/2377–2017) was adopted by the government of Sichuan to tackle the elevated anthropogenic VOCs emissions. As a result, the VOC emissions followed an evenly paced reduction with a prominently descending trend (−5.9% yr^{-1}) throughout 2017–2020. More specifically, anthropogenic VOC emissions are dominated by industrial (228.3 kt), transportation (125.7 kt), and residential sectors (50.7 kt), which account for 56.4%, 31.1%, and 12.5% of total emissions in 2013, respectively. It is important to note that contributions of residential and transportation sectors continuously decreased from 2013 to 2017 (8.4% and 25.5%, respectively in 2017), while the contribution from industrial sector increased to 66.5% in 2017 and maintained as the largest source over 2018–2020. Indeed, the industrial sector is the major source of VOC emissions as well as the driver of total emissions changes (Fig. 5), which highlights the importance of controlling industrial VOC emissions over Chengdu. It is worth mentioning that anthropogenic VOC emissions derived from MEIC lie

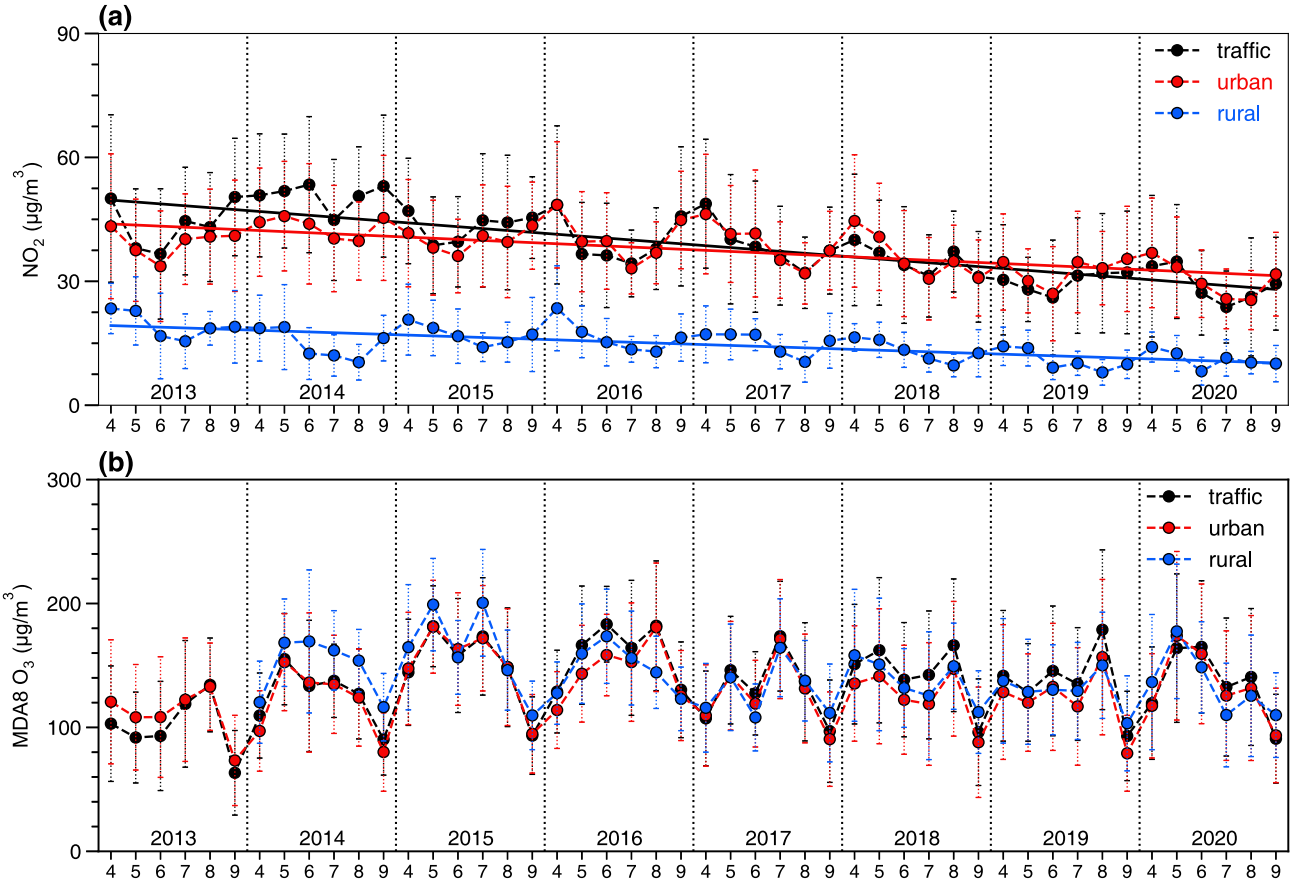

Fig. 3. Monthly averaged concentration of daytime NO_2 and MDA8 O_3 for traffic, urban and rural sites over April–September in Chengdu during 2013–2020.

remarkably close to estimations from Sichuan Academy of Environmental Sciences (Xu et al., 2020) and Simayi et al. (2020), supporting the reliability and robustness of MEIC inventory.

3.3. O_3-VOCs-NO_x sensitivity over Chengdu

3.3.1. Trend of NO_2 and HCHO columns

Uncertainties in bottom-up emission inventory limit the capability of probing accurate emission changes. Here, we further examine the changes of NO_x and VOCs emissions over time by using satellite-derived NO_2 and HCHO columns. The comparison is shown in Fig. S4 with an extended period from 2010 to 2020. Furthermore, the spatial distribution of NO_2 columns observed by OMI and TROPOMI are presented in Fig. 7 and Fig. 8, respectively. Despite the discrepancy in 2014, the trend in OMI NO_2 columns closely tracks the NO_x emissions from MEIC inventory and accurately captures the decrease of NO_x emissions (−3.7%

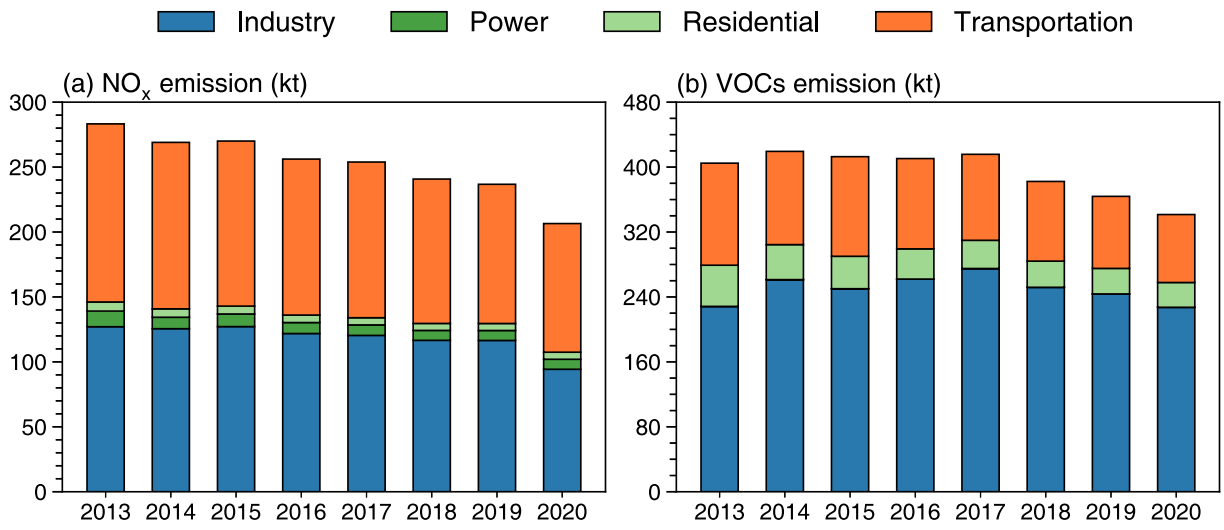

Fig. 4. Anthropogenic NO_x and VOCs emissions in Chengdu by source category for 2013–2020.

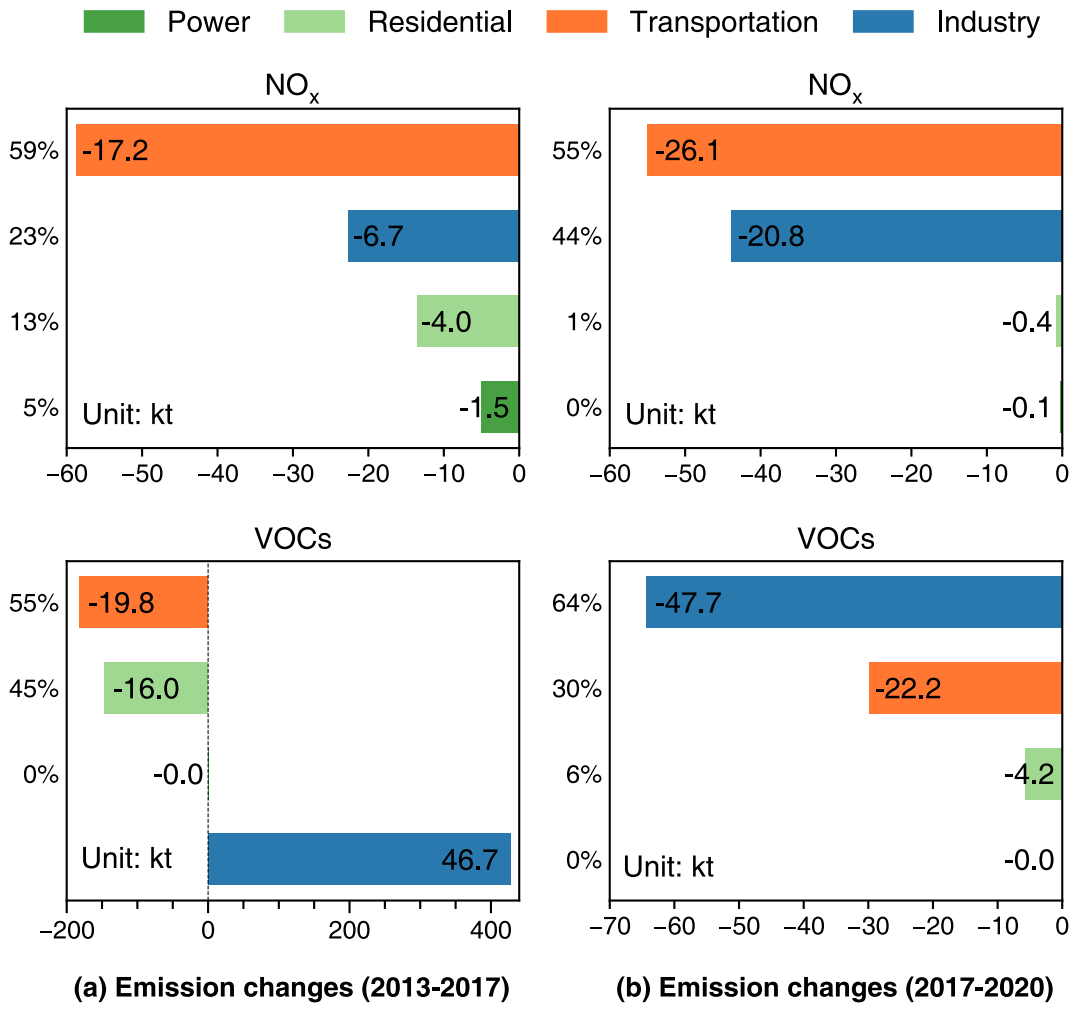

Fig. 5. Emission changes of NO_x and VOCs attributed to each anthropogenic sector for (a) 2013–2017 and (b) 2017–2020.

yr^{-1}) with a steeper trend (−4.5% yr^{-1}) during 2013–2020. This steeper slope has also been found by Shah et al. (2020) over central-eastern China, which might be related to the changes of NO_x lifetime due to decrease in NO_x emissions and meteorological variabilities. The OMI NO_2 columns exhibited a steady decrease since 2014, especially for the metropolitan and suburban areas over Chengdu with a more pronounced trend than the SCB (−3.1% yr^{-1}) (Wu et al., 2022), suggesting successful regulation efforts in reducing anthropogenic NO_x emissions in Chengdu. Interestingly, OMI NO_2 columns in metropolitan Chengdu in 2020 are slightly higher than in 2019, which could be attributed to the economic rebound after COVID-19 lockdown. It is worth noting that the spatial variability and magnitude change of OMI NO_2 column is in excellent agreement with TROPOMI NO_2 columns, and both depict a notable decrease during 2018–2020.

Fig. 9 presents the comparison of anthropogenic and BVOC emissions and OMI HCHO columns during 2010–2020, with the spatial distributions shown in Fig. S5-S6. Following Bauwens et al. (2022) and Shen et al. (2019), the impacts of temperature variabilities on HCHO columns were eliminated by regressing the HCHO columns onto monthly averaged daily maximum 2 m-temperature from the WRF model in each model grid, then the fitted temperature dependency is subtracted from the original data. The temperature-correction algorithm is detailed in Zhu et al. (2017). A weaken correlation is depicted between HCHO columns and BVOC emissions by surmounting temperature dependence. The corrected OMI HCHO columns show a downward trend (−1.7% yr^{-1}) with obvious fluctuations during 2010–2020. In the period from 2010 to 2017, despite the inconspicuous increase of anthropogenic VOC emissions (+1.7% yr^{-1}), the HCHO columns illustrate a descending trend (−1.6% yr^{-1}) with large interannual variability, which could be attributed to significant variations of BVOC emissions. In contrast, the reduction rate of HCHO columns (−6.0% yr^{-1}) is coincident with the decline of anthropogenic VOC emissions (−5.4% yr^{-1}) during 2018–2020, indicating that the reduction of anthropogenic VOC emissions may act as the major driver for the declining HCHO columns since 2018. Furthermore, it is worth noting that a field campaign with an intensive VOCs measurement network over Chengdu was carried out by Tan et al. (2020) in August 2017 to investigate the response of ambient O_3 and precursors levels to short-term strict emission control. It is found that OMI HCHO column decreased by −24.8% during the control period (Fig. S7), which precisely depicted the reductions of ambient VOCs levels ranging from −18.1% to −33.9% based on ground measurements, adding support to the feasibility of inferring trend of VOC emissions using OMI HCHO columns. Overall, both the regulation of anthropogenic VOCs since August 2017 and BVOC emissions modulated by meteorological conditions present essential roles in determining the trend of HCHO columns, which makes Chengdu a notable exception with a negative trend while the trends observed over China are mostly positive (Bauwens et al., 2022). Spatially, apart from the metropolitan area, the elevated HCHO columns were also observed at the northeastern Chengdu (Fig. S6). This phenomenon could be attributed to the local oil refinery industry "China Petroleum Sichuan Petrochemical Corporation" which contributes approximately 8.9 kt VOC emissions

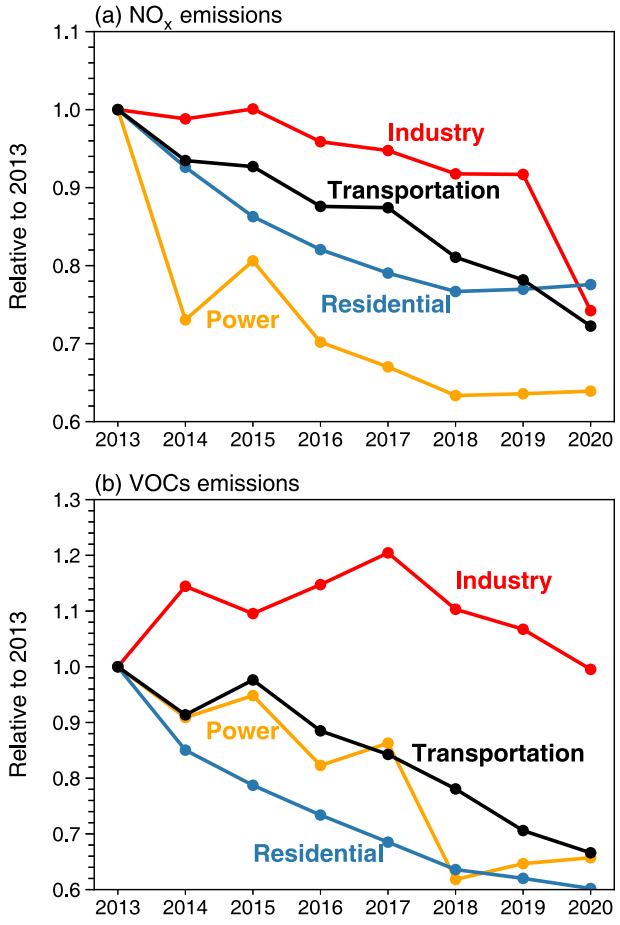

Fig. 6. Trends of NO_x and VOCs emissions for each anthropogenic sector during 2013–2020. The trends are normalized to a value of 1 in 2013.

each year. It should be noted that the changes between VOC emissions and HCHO columns are inconsistent during 2012–2013 and 2017–2018. Possible reasons for these discrepancies including uncertainty in emission inventory and satellite retrievals, as well as the potential impact of meteorological variability (Shah et al., 2020). However, detailed causes of this phenomenon warrant further investigation.

3.3.2. FNR and O_3 concentrations

Fig. 10 presents monthly averaged MDA8 O_3 concentrations plotted against OMI HCHO/NO_2 (FNR) for all environmental monitoring sites during 2013–2020. Following the method developed by Jin et al. (2020), a third-order polynomial model is used to fit the data with a high correlation coefficient ($R = 0.75$), and the transitional regime is defined as the top 20% of the fitted curve. This model clearly captures the nonlinearities in O_3 chemistry with MDA8 O_3 concentration peaks at FNR = 2.75, and the FNR of transitional regime is ranging from 2.27 to 3.26. As NO_2 columns decreased over time, the ratio of HCHO to NO_2 columns continuously increased from 2014 to 2016, indicating that the extent of VOCs-limited regime gradually shrunk in Chengdu (Fig. 11). In terms of MDA8 O_3 concentrations, the urban and traffic sites present steady increasing trends (+13.2% yr^{-1}) during 2013–2016, while a sharp decrease of O_3 concentration (−10.0% yr^{-1}) was observed at rural site in 2016. Furthermore, we also found a strong urban-rural gradients of FNR in 2016, indicating that the metropolitan area of Chengdu remains VOCs-limited regime, while the rural area has shifted from VOCs-limited to transitional or NO_x-limited in 2016 (Fig. 12). Interestingly, the average O_3 concentration decreased by 14.0% from 2016 to 2017, and then rebounded in 2018. The reason for this drop could be inferred from the consistent decreasing trends of BVOC emissions and HCHO columns combined with the expansion of VOCs-limited regime in 2017, indicating that the reductions of BVOC emissions which are modulated by meteorological variability play a crucial role in the decrease of O_3 levels. After 2017, the anthropogenic NO_x and VOC emissions are jointly regulated, and the decreasing trends of NO_2 and HCHO columns are identified over 2018–2020. These emission regulations resulted in the decrease of O_3 concentrations at all monitoring sites from 2018 to 2019, while the O_3 levels were observed to slightly increase in 2020, which should be linked to the unfavorable meteorological conditions in 2020 (discussed in Section 3.4).

3.3.3. Trend of O_3-VOCs-NO_x sensitivity

Compared with the O_3-VOCs-NO_x sensitivity of Chengdu reported in previous studies (Table 1), our results are generally consistent with them. Before the implementation of emission controls, the extent of transitional and VOC-limited regime continuously extended due to the rapid increase of NO_x emissions from 2005, and most areas of Chengdu have been characterized as VOC-limited in 2013 (Jin and Holloway, 2015). During 2013–2020, we found the urban area remains at VOC-limited regime, which is further verified by existing evidence from field measurement and chemical transport models (CTMs). For instance, Tan et al. (2018) found the negative effect of NO_x reduction on O_3 control by conducting field measurements combined with a box model (OBM) in 2016. Based on the O_3 isopleth derived from the CMAQ model, Shen et al. (2021) reported that Chengdu city metropolitan area shows a NO_x-saturated O_3 regime, where the O_3 production was sensitive to VOC emissions in 2017. Han et al. (2020) also revealed that O_3 formation had negative sensitivity to NO_x over urban Chengdu in 2019. For suburban areas, Deng et al. (2019) carried out the field measurement at the central north suburb of Chengdu (Pixian district: black circle in Fig. 12b), and reported that the sampling site is under VOC-limited in 2016, while the north suburb of Chengdu (Pengzhou district: black pentagram in Fig. 12b) is identified as transitional regime (Tan et al., 2018). The discrepancy between these two studies is linked to the elevated VOC emissions from local petroleum industry in Pengzhou. In particular, when compared to a recent study by Du et al. (2022), which also explored the spatial distribution of O_3-VOCs-NO_x sensitivity from June to September in 2019 over Chengdu by using the comprehensive air quality model with extensions (CAMx)-high-order decoupled direct method (HDDM). The O_3 formation sensitivity inferred by OMI HCHO/NO_2 is consistent with their results, both clearly present the shift of VOC-limited to transitional or NO_x-limited between urban and suburban areas. These studies illustrate the complex variabilities of O_3-VOCs-NO_x sensitivity over the Chengdu city. Therefore, future work should consider using more comprehensive field measurements and numerical models to quantitatively identify the most effective reduction magnitude for jointly controlling of NO_x and VOC emissions to improve O_3 pollution over Chengdu.

3.4. Relationship between O_3 variability and meteorological conditions

Heatwaves and stagnant events are the most critical meteorological phenomenon that governs variations in O_3 levels (Yang and Shao, 2021). Fig. S8 shows the monthly occurrence frequencies of HWs and stagnation derived from the WRF model, as well as their co-occurrence over 2013–2020. There is a high probability of HWs occurrence in summer, with peak frequency in July. The similar feature was also found in the earlier work by Huang et al. (2021) for SCB. In terms of the air stagnation, our result shows relatively less occurrence in July and August, which could be attributed to the frequent rainfalls over the SCB in summer (Qian et al., 2015). Over the warm season, the co-occurrence frequencies of stagnant conditions and HWs ranging from 1.2% to 4.6% for the whole city during 2013–2020, and Chengdu is most susceptible to HWs and stagnant in 2019 and 2020, with co-occurrence frequencies higher than 8.0% at the metropolitan area (Fig. S9), indicating that the HWs and stagnant conditions might become more

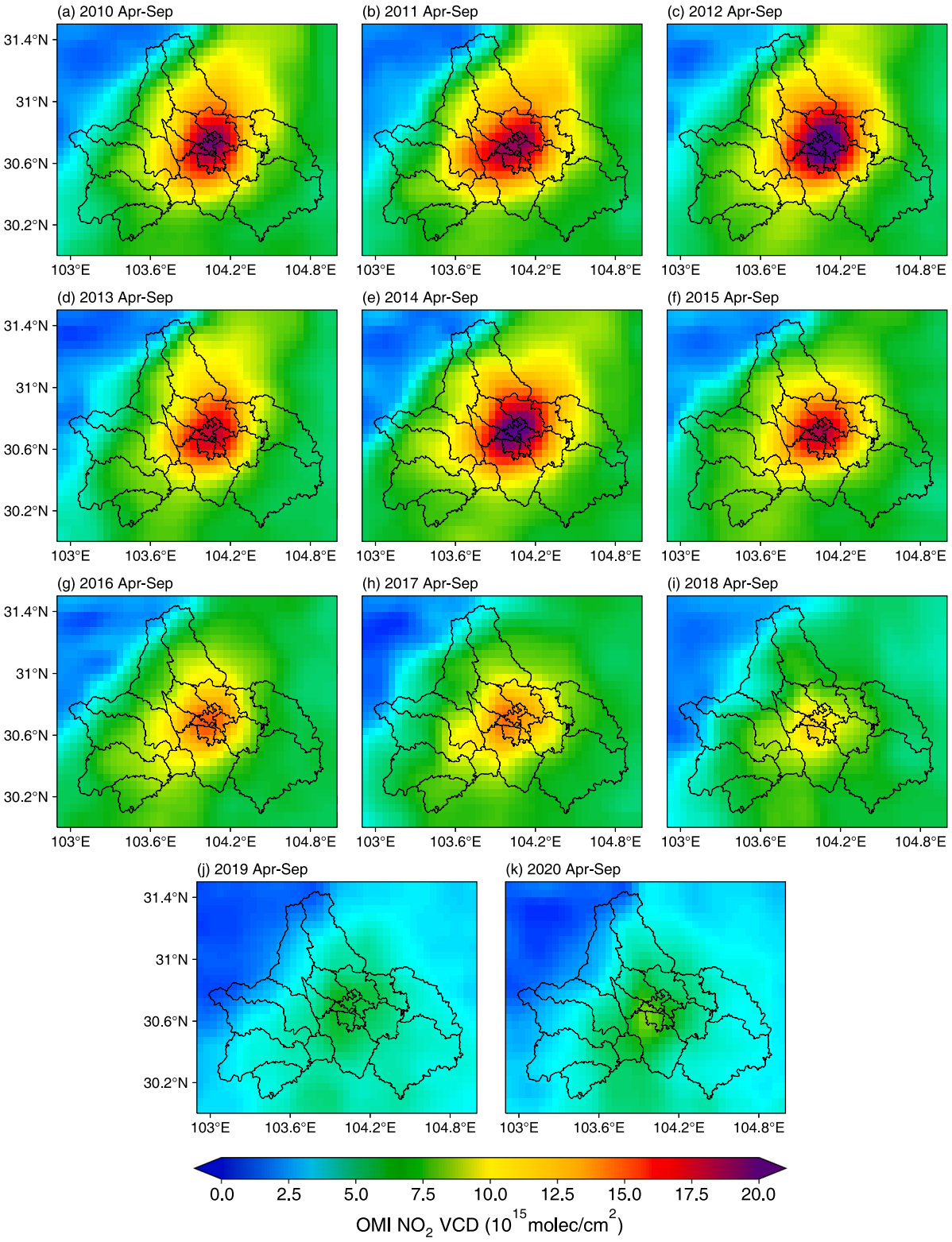

Fig. 7. OMI NO_2 vertical column densities averaged over a 6-month period April–September from 2010 to 2020 in Chengdu.

frequent under the changing climate.

By comparing the trends of extreme meteorological events and O_3 levels, we find a high degree of correlation between monthly O_3 variations and the occurrence of HWs and stagnation over Chengdu. Fig. 13 depicts several periods that abovementioned meteorological phenomenon could well explain anomalous high or low O_3 levels over time. Specifically, enhanced rural O_3 levels in July 2015 are closely associated with frequent stagnations over rural areas (frequency in excess of 30%). Similarly, elevated O_3 levels in June and August in 2016 are clearly linked to profound HWs (frequency higher than 30%) occurrence during the period which triggered intense photochemical reactions. Furthermore, severe O_3 pollution in August 2019 is largely determined by the

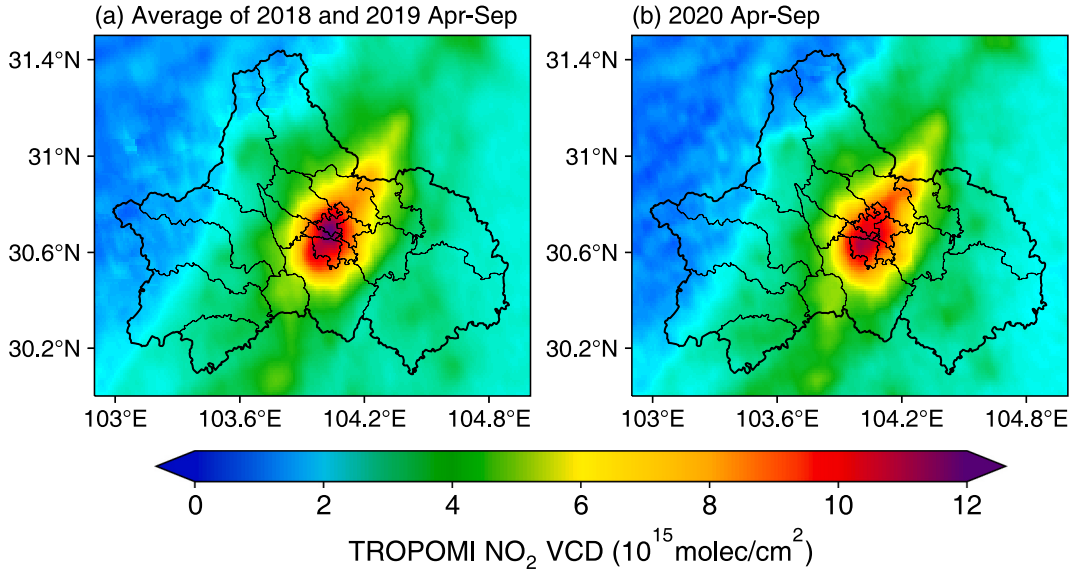

Fig. 8. TROPOMI NO_2 vertical column densities averaged over a 6-month period April–September from 2018 to 2020.

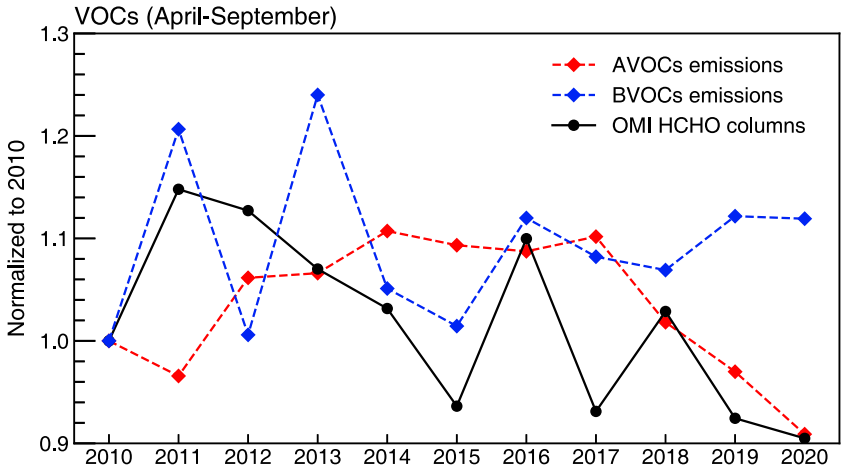

Fig. 9. The trends of anthropogenic VOCs (AVOCs) and biogenic VOCs (BVOCs) emissions and corrected OMI HCHO columns over April–September in Chengdu during 2010–2020. The trends are normalized to a value of 1 in 2010.

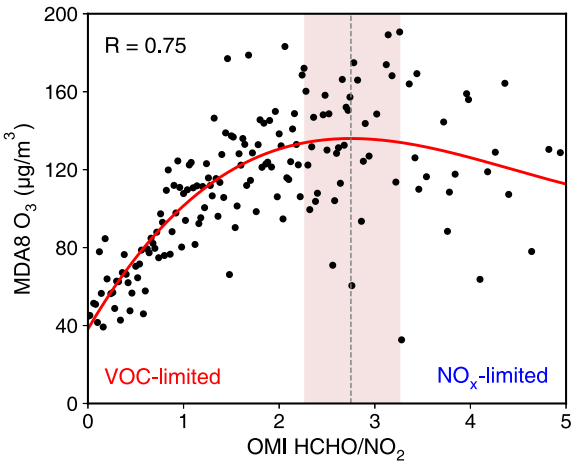

Fig. 10. Monthly averaged MDA8 O_3 concentrations are plotted against OMI HCHO/NO_2 for all environmental monitoring sites during 2013–2020. The solid lines are fitted third-order polynomial curve. The shaded area represents the range over the top 20% of the fitted curve (transitional regime).

co-occurrence of stagnant conditions and HWs (Fig. 13f). It is worth noting that the most prominent period that O_3 was affected by meteorological fields is May 2020. Fig. S10 presents the changes of simulated daytime 2-m temperature and precipitation in May 2020 relative to May 2019. The temperature increase (>4 °C) was also coincident with a sharp drop in precipitation (up to 60 mm or 35% reduction) over Chengdu in May 2020 compared with May 2019, while anthropogenic emissions of NO_x and VOCs reduced by 11.3% and 6.3% in Chengdu due to Covid-19 lockdown, respectively. Such a strong warming magnitude combined with droughty condition caused Chengdu endures profound heatwaves and air stagnations in May 2020, subsequently leading to numerous O_3 exceedances (as reflected by the spike in O_3 levels). This opposed phenomenon demonstrates the considerable contribution of persistent unfavorable meteorological fields on elevating O_3 concentrations which could even fully offset the effects of emission reductions. This is in agreement with Sun et al. (2021) and Wu et al. (2022), who use chemical transport models to quantitively identify the role of unprecedented meteorological phenomenon on high levels of O_3 in May 2020.

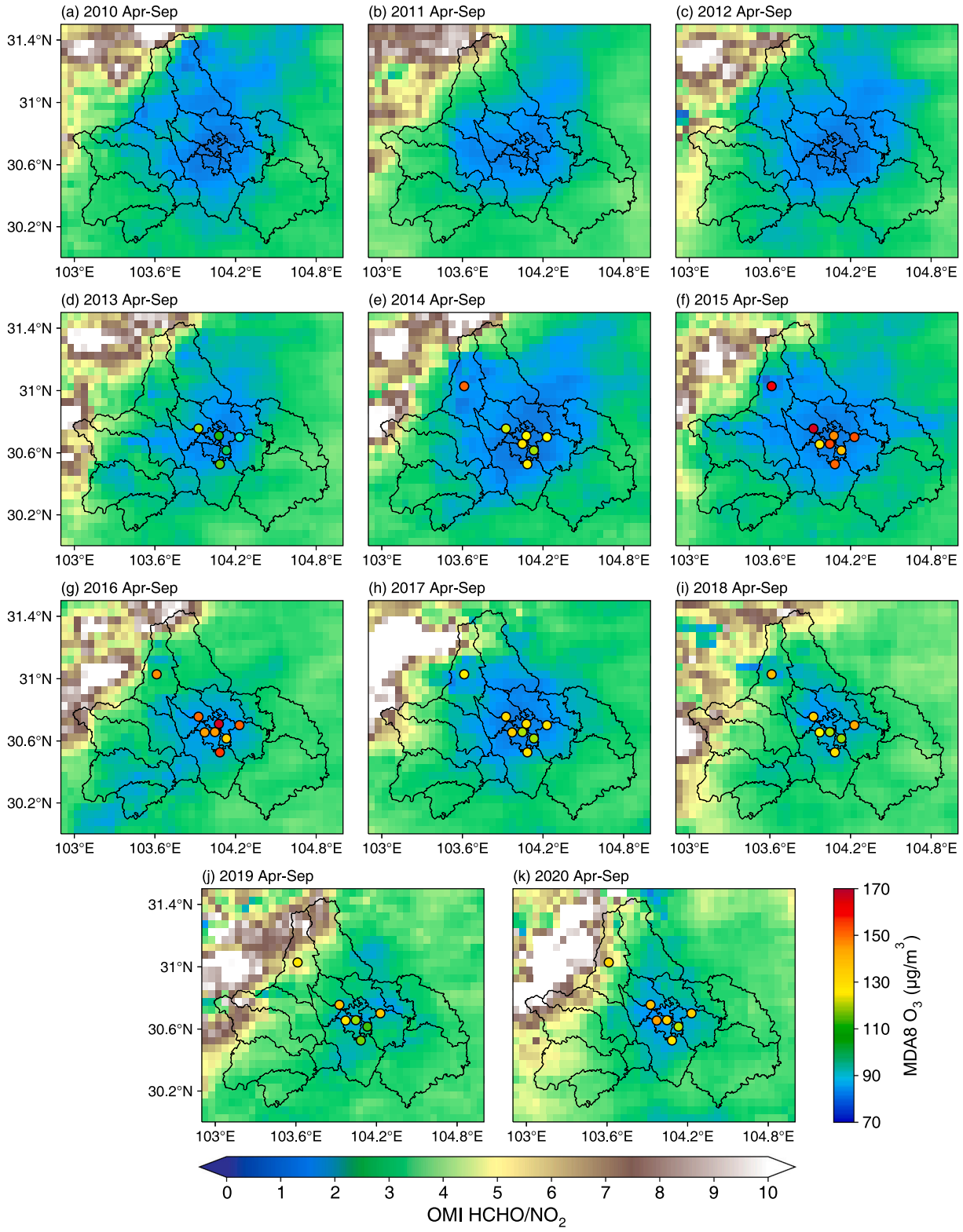

Fig. 11. Map of $HCHO/NO_2$ (FNR) and O_3 levels averaged over a 6-month period April–September from 2010 to 2020 over Chengdu.

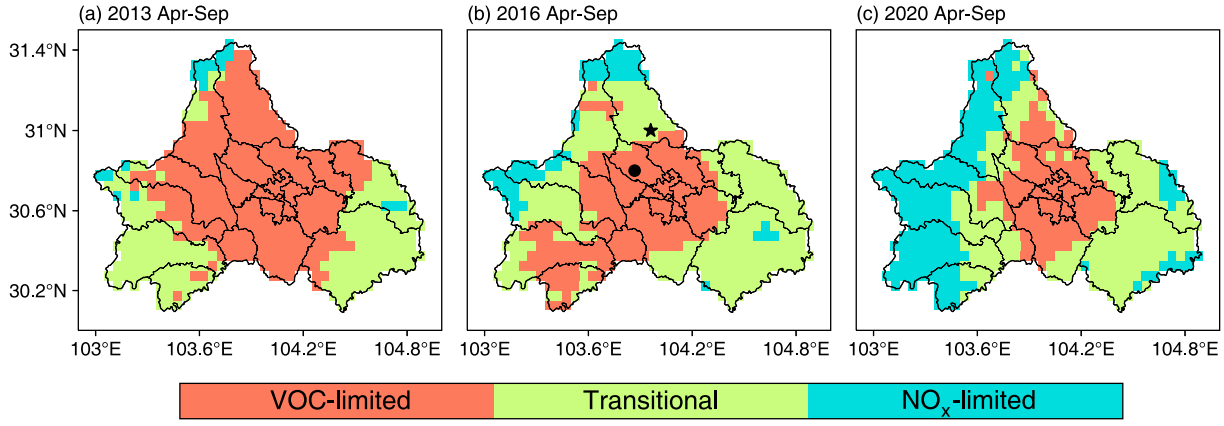

Fig. 12. O_3-VOCs-NO_x sensitivity inferred by OMI HCHO/NO_2 over a 6-month period April–September in 2013, 2016 and 2020 in Chengdu. In 2016, the black circle site is reported in VOC-limited regime (Deng et al., 2019), while the pentagram is in transitional regime (Tan et al., 2018).

Table 1
Comparisons of previous O_3-VOCs-NO_x sensitivity over Chengdu.

Area	Period	O_3-VOCs-NO_x sensitivity	Method	Reference
Urban	2005	transitional or NO_x-limited	FNR from OMI	Jin and Holloway (2015)
	Mar, 2010	transitional or VOC-limited	WRF-CALGRID	Xie et al. (2014)
	2013	transitional or VOC-limited	FNR from OMI	Jin and Holloway (2015)
	Sep, 2016	VOC-limited	box model (OBM)	Tan et al. (2018)
	Aug-Sep, 2017	VOC-limited	field measurement	Tan et al. (2020)
	2017	VOC-limited	CMAQ model	Shen et al. (2021)
	Apr-Aug, 2019	VOC-limited	OBM	Han et al. (2020)
	Jun-Sep, 2019	VOC-limited	CAMx-HDDM model	Du et al. (2022)
	2013–2020	VOC-limited	FNR and field measurement	This study
Suburban	Aug-Oct, 2016	VOC-limited	field measurement	Deng et al. (2019)
	Sep, 2016	transitional	OBM	Tan et al. (2018)
	Jun-Sep, 2019	transitional or NO_x-limited	CAMx-HDDM model	Du et al. (2022)
Rural	2013–2015	VOC-limited	FNR and field measurement	This study
	2016–2020	transitional or NO_x-limited	FNR and field measurement	This study

4. Conclusion

Long-term O_3 and precursor observations from 2013 to 2020 in Chengdu, a megacity located in southwestern China, have provided insight into the changes of ambient O_3 and precursors levels in response to regulation efforts. We depicted deteriorated O_3 trends ($+14.0\%\ yr^{-1}$) at urban and traffic sites during 2013–2016 followed by a weak reduction with notable interannual variability afterwards. In contrast, O_3 concentration at rural areas generally shows a downward trend ($-2.9\%\ yr^{-1}$) during 2014–2020. Further analysis based on MEIC inventory ($-3.7\%\ yr^{-1}$) and OMI NO_2 columns ($-4.5\%\ yr^{-1}$) reported strong evidence on the continuous reductions in NO_x emission from 2013 to 2020. However, OMI HCHO columns exhibit a weaker declining trend over time, with the most notable decrease in 2018–2020 ($-6.0\%\ yr^{-1}$), implying the effectiveness of targeted legislature concerning VOC emissions in Chengdu. Noticing the discrepancies between the trends of NO_x and VOC emissions, which could lead to dramatic changes in O_3-VOCs-NO_x sensitivity, we further analyze the relationship between FNR and field measurements to probe the transition of O_3-VOCs-NO_x sensitivity over Chengdu. The results indicate that metropolitan Chengdu remains VOCs-limited regime during 2013–2020, while the rural area has shifted from VOCs-limited to transitional or NO_x-limited regime since 2016. Given the well-supported identification of O_3-VOCs-NO_x sensitivity, it is expected that the emission regulation framework involves joint control of NO_x and VOC emissions would lead to evident O_3 improvements in near future. Nevertheless, the variabilities of meteorological phenomenon and biogenic emissions should not be neglected, as modeling results indicate that extreme unfavorable meteorological conditions accompanied by enhanced BVOC emissions in a short period (May 2020) could even fully offset O_3 benefits over warm season. Thus, the potential perturbation induced by meteorological phenomenon and BVOC emissions under warming climate deserves further study for ensuring the effectiveness of O_3 abatement strategy not overestimated.

Recent studies have noted the steady reductions of NO_x emissions from 2013 throughout China attributed to regulation efforts introduced by APPCAP, but changes in anthropogenic VOCs emissions remain uncertain, particularly in highly urbanized megacities. Our analysis provides robust evidence derived from both emission inventory and satellite data which points to the success in reducing NO_x emissions since 2013 and cutting VOCs emissions after 2017 in Chengdu. However, the response of ambient O_3 levels is relatively weak due to the gradual transition of O_3-VOCs-NO_x regime and increased emissions of biogenic precursors under a warming climate. Furthermore, the projected expansion in urban green spaces attributed to the implementation of

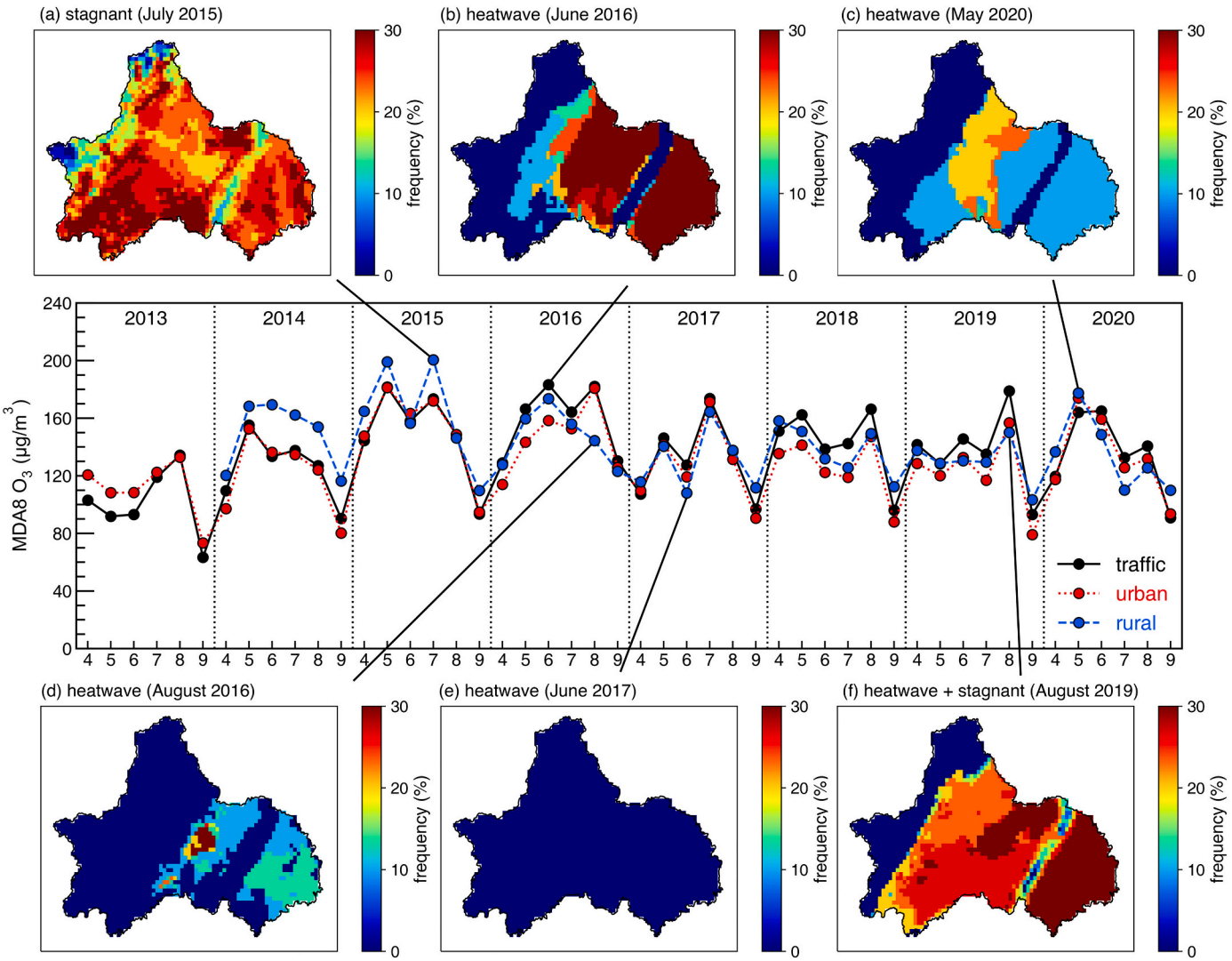

Fig. 13. (Middle panel) Monthly average concentration of MDA8 O_3 for traffic, urban and rural stations for April–September from 2013 to 2020, and occurrence frequency maps of heatwave and stagnant of extreme meteorological events over Chengdu.

urban greening strategies could result in substantial BVOC emissions in urban areas, thus posing challenges to O_3 regulation (Gu et al., 2021). While meteorological phenomena and enhanced BVOC emissions likely obscured the expected decline in O_3 concentrations, ongoing control strategies involving joint regulation of NO_x and VOCs would be increasingly effective in controlling O_3 pollution in Chengdu. This work may also be compelling to megacities in East Asia where anthropogenic emissions undergo similar pathways as Chengdu. Although the abundance of precursor emissions may differ slightly among megacities, this work provides an improved scientific basis for diagnosing O_3 variability and associated driving factors over time, thus showing important implications in developing reliable emission control strategies toward compliance of O_3 air quality standards.

CRediT authorship contribution statement

Yurun Wang: Writing – original draft, Conceptualization, Methodology, Software. **Xianyu Yang:** Writing – review & editing, Supervision, Project administration. **Kai Wu:** Methodology, Software, Formal analysis, Writing – review & editing. **Han Mei:** Software, Writing – review & editing. **Isabelle De Smedt:** Writing – review & editing, Methodology, Software. **Shigong Wang:** Supervision, Project administration, Funding acquisition. **Jin Fan:** Writing – review & editing. **Shihua Lyu:** Supervision, Project administration, Funding acquisition. **Cheng He:** Writing – review & editing.

Declaration of Competing Interest

The authors declare that they have no known competing financial interests or personal relationships that could have appeared to influence the work reported in this paper.

Acknowledgments

The authors acknowledge the MEIC team and Dr. Bo Zheng from Tsinghua University for providing the Multi-resolution Emission Inventory for China (MEIC) and Chengdu Plain Urban Meteorology and Environment Observation and Research Station of Sichuan Province for providing ambient monitoring data. This work was funded by the National Natural Science Foundation of China (No.42175174, No.42105167), Open Research Fund Program of Plateau Atmosphere and Environment Key Laboratory of Sichuan Province (No.PAEKL-2020-C6), and the Scientific Research Foundation of the Chengdu University of Information Technology (No.KYTZ201823). The authors thank EU FP7 QA4ECV project (No.607405) for providing OMI NO_2 and HCHO column data. This work contains modified Copernicus Sentinel-5

Precursor satellite data (2018–2020). The data used in this work is available from the corresponding author upon reasonable request.

Appendix A. Supplementary data

Supplementary data to this article can be found online at https://doi.org/10.1016/j.atmosres.2022.106309.

References

Bauwens, M., Verreyken, B., Stavrakou, T., Müller, J.-F., Smedt, I.D., 2022. Spaceborne evidence for significant anthropogenic VOC trends in Asian cities over 2005–2019. Environ. Res. Lett. 17, 015008 https://doi.org/10.1088/1748-9326/ac46eb.

Boersma, K.F., Eskes, H.J., Richter, A., De Smedt, I., Lorente, A., Beirle, S., van Geffen, J. H.G.M., Zara, M., Peters, E., Van Roozendael, M., Wagner, T., Maasakkers, J.D., van der, A.R.J., Nightingale, J., De Rudder, A., Irie, H., Pinardi, G., Lambert, J.-C., Compernolle, S.C., 2018. Improving algorithms and uncertainty estimates for satellite NO2 retrievals: results from the quality assurance for the essential climate variables (QA4ECV) project. Atmos. Meas. Tech. 11, 6651–6678. https://doi.org/10.5194/amt-11-6651-2018.

Chen, Y., Han, H., Zhang, M., Zhao, Y., Huang, Y., Zhou, M., Wang, C., He, G., Huang, R., Luo, B., Hu, Y., 2021. Trends and variability of ozone pollution over the mountain-basin areas in Sichuan Province during 2013–2020: synoptic impacts and formation regimes. Atmosphere 12, 1557. https://doi.org/10.3390/atmos12121557.

Cohen, A.J., Brauer, M., Burnett, R., Anderson, H.R., Frostad, J., Estep, K., Balakrishnan, K., Brunekreef, B., Dandona, L., Dandona, R., Feigin, V., Freedman, G., Hubbell, B., Jobling, A., Kan, H., Knibbs, L., Liu, Y., Martin, R., Morawska, L., Pope, C.A., Shin, H., Straif, K., Shaddick, G., Thomas, M., van Dingenen, R., van Donkelaar, A., Vos, T., Murray, C.J.L., Forouzanfar, M.H., 2017. Estimates and 25-year trends of the global burden of disease attributable to ambient air pollution: an analysis of data from the global burden of diseases study 2015. Lancet 389, 1907–1918. https://doi.org/10.1016/S0140-6736(17)30505-6.

De Smedt, I., Theys, N., Yu, H., Danckaert, T., Lerot, C., Compernolle, S., Van Roozendael, M., Richter, A., Hilboll, A., Peters, E., Pedergnana, M., Loyola, D., Beirle, S., Wagner, T., Eskes, H., van Geffen, J., Boersma, K.F., Veefkind, P., 2018. Algorithm theoretical baseline for formaldehyde retrievals from S5P TROPOMI and from the QA4ECV project. Atmos. Meas. Tech. 11, 2395–2426. https://doi.org/10.5194/amt-11-2395-2018.

De Smedt, I., Pinardi, G., Vigouroux, C., Compernolle, S., Bais, A., Benavent, N., Boersma, F., Chan, K.-L., Donner, S., Eichmann, K.-U., Hedelt, P., Hendrick, F., Irie, H., Kumar, V., Lambert, J.-C., Langerock, B., Lerot, C., Liu, C., Loyola, D., Piters, A., Richter, A., Rivera Cárdenas, C., Romahn, F., Ryan, R.G., Sinha, V., Theys, N., Vlietinck, J., Wagner, T., Wang, T., Yu, H., Van Roozendael, M., 2021. Comparative assessment of TROPOMI and OMI formaldehyde observations and validation against MAX-DOAS network column measurements. Atmos. Chem. Phys. 21, 12561–12593. https://doi.org/10.5194/acp-21-12561-2021.

Deng, Y., Li, J., Li, Y., Wu, R., Xie, S., 2019. Characteristics of volatile organic compounds, NO2, and effects on ozone formation at a site with high ozone level in Chengdu. J. Environ. Sci. 75, 334–345. https://doi.org/10.1016/j.jes.2018.05.004.

Du, X., Tang, W., Zhang, Z., Li, Y., Yu, Y., Xiao, Z., Meng, F., 2022. Sensitivity modeling of ozone and its precursors over the Chengdu metropolitan area. Atmos. Environ. 277, 119071 https://doi.org/10.1016/j.atmosenv.2022.119071.

Duncan, B.N., Yoshida, Y., Olson, J.R., Sillman, S., Martin, R.V., Lamsal, L., Hu, Y., Pickering, K.E., Retscher, C., Allen, D.J., Crawford, J.H., 2010. Application of OMI observations to a space-based indicator of NOx and VOC controls on surface ozone formation. Atmos. Environ. 44, 2213–2223. https://doi.org/10.1016/j.atmosenv.2010.03.010.

Gao, H., Yang, W., Wang, J., Zheng, X., 2020. Analysis of the effectiveness of air pollution control policies based on historical evaluation and deep learning forecast: a case study of Chengdu-Chongqing region in China. Sustainability 13, 206. https://doi.org/10.3390/su13010206.

Gao, W., Tie, X., Xu, J., Huang, R., Mao, X., Zhou, G., Chang, L., 2017. Long-term trend of O3 in a mega City (Shanghai), China: Characteristics, causes, and interactions with precursors. Sci. Total Environ. 603–604, 425–433. https://doi.org/10.1016/j.scitotenv.2017.06.099.

van Geffen, J., Boersma, K.F., Eskes, H., Sneep, M., ter Linden, M., Zara, M., Veefkind, J. P., 2020. S5P TROPOMI NO2 slant column retrieval: method, stability, uncertainties and comparisons with OMI. Atmos. Meas. Tech. 13, 1315–1335. https://doi.org/10.5194/amt-13-1315-2020.

Gu, S., Guenther, A., Faiola, C., 2021. Effects of anthropogenic and biogenic volatile organic compounds on los angeles air quality. Environ. Sci. Technol. 55, 12191–12201. https://doi.org/10.1021/acs.est.1c01481.

Guenther, A.B., Jiang, X., Heald, C.L., Sakulyanontvittaya, T., Duhl, T., Emmons, L.K., Wang, X., 2012. The Model of Emissions of gases and Aerosols from Nature version 2.1 (MEGAN2.1): an extended and updated framework for modeling biogenic emissions. Geosci. Model Dev. 5, 1471–1492. https://doi.org/10.5194/gmd-5-1471-2012.

Han, L., Chen, J., Jiang, T., et al., 2020. Sensitivity analysis of atmospheric ozone formation to its precursors in Chengdu with an observation based model [J]. Acta Sci. Circumst. 40 (11), 4092–4104.

He, Z., Wang, X., Ling, Z., Zhao, J., Guo, H., Shao, M., Wang, Z., 2019. Contributions of different anthropogenic volatile organic compound sources to ozone formation at a receptor site in the Pearl River Delta region and its policy implications. Atmos. Chem. Phys. 19, 8801–8816. https://doi.org/10.5194/acp-19-8801-2019.

Horton, D.E., Harshvardhan, Diffenbaugh, N.S., 2012. Response of air stagnation frequency to anthropogenically enhanced radiative forcing. Environ. Res. Lett. 7, 044034 https://doi.org/10.1088/1748-9326/7/4/044034.

Huang, X., Zhang, T., Jiang, X., Liu, S., Xiao, D., 2021. Interannual variability of mid-summer heat wave frequency over the Sichuan Basin. Int. J. Climatol. 41, 5036–5050. https://doi.org/10.1002/joc.7115.

Jin, X., Holloway, T., 2015. Spatial and temporal variability of ozone sensitivity over China observed from the ozone monitoring instrument. J. Geophys. Res. Atmos. 120, 7229–7246. https://doi.org/10.1002/2015JD023250.

Jin, X., Fiore, A., Boersma, K.F., Smedt, I.D., Valin, L., 2020. Inferring changes in summertime surface ozone–NOx–VOC chemistry over U.S. Urban areas from two decades of satellite and ground-based observations. Environ. Sci. Technol. 54, 6518–6529. https://doi.org/10.1021/acs.est.9b07785.

Kalabokas, P., Hjorth, J., Foret, G., Dufour, G., Eremenko, M., Siour, G., Cuesta, J., Beekmann, M., 2017. An investigation on the origin of regional springtime ozone episodes in the western Mediterranean. Atmos. Chem. Phys. 17, 3905–3928. https://doi.org/10.5194/acp-17-3905-2017.

Li, M., Liu, H., Geng, G., Hong, C., Liu, F., Song, Y., Tong, D., Zheng, B., Cui, H., Man, H., Zhang, Q., He, K., 2017. Anthropogenic emission inventories in China: a review. Natl. Sci. Rev. 4, 834–866. https://doi.org/10.1093/nsr/nwx150.

Liu, H., Liu, S., Xue, B., Lv, Z., Meng, Z., Yang, X., Xue, T., Yu, Q., He, K., 2018. Ground-level ozone pollution and its health impacts in China. Atmos. Environ. 173, 223–230. https://doi.org/10.1016/j.atmosenv.2017.11.014.

Liu, J., Wang, L., Li, M., Liao, Z., Sun, Y., Song, T., Gao, W., Wang, Y., Li, Y., Ji, D., Hu, B., Kerminen, V.-M., Wang, Y., Kulmala, M., 2019. Quantifying the impact of synoptic circulation patterns on ozone variability in northern China from April to October 2013–2017. Atmos. Chem. Phys. 19, 14477–14492. https://doi.org/10.5194/acp-19-14477-2019.

Liu, Y., Wang, T., 2020a. Worsening urban ozone pollution in China from 2013 to 2017 – part 1: the complex and varying roles of meteorology. Atmos. Chem. Phys. 20, 6305–6321. https://doi.org/10.5194/acp-20-6305-2020.

Liu, Y., Wang, T., 2020b. Worsening urban ozone pollution in China from 2013 to 2017 – part 2: the effects of emission changes and implications for multi-pollutant control. Atmos. Chem. Phys. 20, 6323–6337. https://doi.org/10.5194/acp-20-6323-2020.

Lyu, X., Wang, N., Guo, H., Xue, L., Jiang, F., Zeren, Y., Cheng, H., Cai, Z., Han, L., Zhou, Y., 2019. Causes of a continuous summertime O3 pollution event in Jinan, a central city in the North China Plain. Atmos. Chem. Phys. 19, 3025–3042. https://doi.org/10.5194/acp-19-3025-2019.

Ma, M., Gao, Y., Ding, A., Su, H., Liao, H., Wang, S., Wang, X., Zhao, B., Zhang, S., Fu, P., Guenther, A.B., Wang, M., Li, S., Chu, B., Yao, X., Gao, H., 2022. Development and assessment of a high-resolution biogenic emission inventory from urban green spaces in China. Environ. Sci. Technol. 56, 175–184. https://doi.org/10.1021/acs.est.1c06170.

Meng, X., Pang, K., Yin, Z., Xiang, X., 2021. Grid-based spatiotemporal modeling of ambient ozone to assess human exposure using environmental big data. Atmos. Pollut. Res. 12, 101216 https://doi.org/10.1016/j.apr.2021.101216.

Ministry of Ecology and Environment (MEE) of the People"s Republic of China, 2012. Ambien Air Quality Standards (GB 3095–2012). http://218.108.6.124:8099/aqms/download/GB3095-2012.pdf.

Ministry of Ecology and Environment (MEE) of the People"s Republic of China, 2018. Revision of the Ambien Air Quality Standards (GB 3095-2012). http://www.mee.gov.cn/xxgk2018/xxgk/xxgk01/201808/t20180815_629602.html (in Chinese).

Orru, H., Andersson, C., Ebi, K.L., Langner, J., Åström, C., Forsberg, B., 2013. Impact of climate change on ozone-related mortality and morbidity in Europe. Eur. Respir. J. 41, 285–294. https://doi.org/10.1183/09031936.00210411.

Qian, T., Zhao, P., Zhang, F., Bao, X., 2015. Rainy-season precipitation over the sichuan basin and adjacent regions in Southwestern China. Mon. Weather Rev. 143, 383–394. https://doi.org/10.1175/MWR-D-13-00158.1.

Shah, V., Jacob, D.J., Li, K., Silvern, R.F., Zhai, S., Liu, M., Lin, J., Zhang, Q., 2020. Effect of changing NOx lifetime on the seasonality and long-term trends of satellite-observed tropospheric NO2 columns over China. Atmos. Chem. Phys. 20, 1483–1495. https://doi.org/10.5194/acp-20-1483-2020.

Shen, H., Sun, Z., Chen, Y., Russell, A.G., Hu, Y., Odman, M.T., Qian, Y., Archibald, A.T., Tao, S., 2021. Novel method for ozone isopleth construction and diagnosis for the ozone control strategy of Chinese cities. Environ. Sci. Technol. https://doi.org/10.1021/acs.est.1c01567 acs.est.1c01567.

Shen, L., Jacob, D.J., Zhu, L., Zhang, Q., Zheng, B., Sulprizio, M.P., Li, K., De Smedt, I., González Abad, G., Cao, H., Fu, T., Liao, H., 2019. The 2005–2016 trends of formaldehyde columns over china observed by satellites: increasing anthropogenic emissions of volatile organic compounds and decreasing agricultural fire emissions. Geophys. Res. Lett. 46, 4468–4475. https://doi.org/10.1029/2019GL082172.

Simayi, M., Shi, Y., Xi, Z., Li, J., Yu, X., Liu, H., Tan, Q., Song, D., Zeng, L., Lu, S., Xie, S., 2020. Understanding the sources and spatiotemporal characteristics of VOCs in the Chengdu Plain, China, through measurement and emission inventory. Sci. Total Environ. 714, 136692 https://doi.org/10.1016/j.scitotenv.2020.136692.

Stowell, J.D., Kim, Y., Gao, Y., Fu, J.S., Chang, H.H., Liu, Y., 2017. The impact of climate change and emissions control on future ozone levels: Implications for human health. Environ. Int. 108, 41–50. https://doi.org/10.1016/j.envint.2017.08.001.

Sun, K., Zhu, L., Cady-Pereira, K., Chan Miller, C., Chance, K., Clarisse, L., Coheur, P.-F., González Abad, G., Huang, G., Liu, X., Van Damme, M., Yang, K., Zondlo, M., 2018. A physics-based approach to oversample multi-satellite, multispecies observations to a common grid. Atmos. Meas. Tech. 11, 6679–6701. https://doi.org/10.5194/amt-11-6679-2018.

Sun, Y., Yin, H., Lu, X., Notholt, J., Palm, M., Liu, C., Tian, Y., Zheng, B., 2021. The drivers and health risks of unexpected surface ozone enhancements over the Sichuan Basin, China, in 2020. Atmos. Chem. Phys. 21, 18589–18608. https://doi.org/10.5194/acp-21-18589-2021.

Tan, Q., Zhou, L., Liu, H., Feng, M., Qiu, Y., Yang, F., Jiang, W., Wei, F., 2020. Observation-based Summer O3 control effect evaluation: a case study in chengdu, a megacity in Sichuan Basin, China. Atmosphere 11, 1278. https://doi.org/10.3390/atmos11121278.

Tan, Z., Lu, K., Jiang, M., Su, R., Dong, H., Zeng, L., Xie, S., Tan, Q., Zhang, Y., 2018. Exploring ozone pollution in Chengdu, southwestern China: a case study from radical chemistry to O3-VOC-NOx sensitivity. Sci. Total Environ. 636, 775–786. https://doi.org/10.1016/j.scitotenv.2018.04.286.

Trainer, M., Parrish, D.D., Goldan, P.D., Roberts, J., Fehsenfeld, F.C., 2000. Review of observation-based analysis of the regional factors influencing ozone concentrations. Atmos. Environ. 17.

Urraca, R., Huld, T., Gracia-Amillo, A., Martinez-de-Pison, F.J., Kaspar, F., Sanz-Garcia, A., 2018. Evaluation of global horizontal irradiance estimates from ERA5 and COSMO-REA6 reanalyses using ground and satellite-based data. Sol. Energy 164, 339–354. https://doi.org/10.1016/j.solener.2018.02.059.

Wang, H., Wu, K., Liu, Y., Sheng, B., Lu, X., He, Y., Xie, J., Wang, H., Fan, S., 2021. Role of heat wave-induced biogenic VOC enhancements in persistent ozone episodes formation in pearl river delta. J. Geophys. Res. Atmos. 126 https://doi.org/10.1029/2020JD034317.

Wang, L., Li, M., Wang, Q., Li, Y., Xin, J., Tang, X., Du, W., Song, T., Li, T., Sun, Y., Gao, W., Hu, B., Wang, Y., 2022. Air stagnation in China: Spatiotemporal variability and differing impact on PM2.5 and O3 during 2013–2018. Sci. Total Environ. 819, 152778 https://doi.org/10.1016/j.scitotenv.2021.152778.

Wang, Y., Wild, O., Chen, X., Wu, Q., Gao, M., Chen, H., Qi, Y., Wang, Z., 2020. Health impacts of long-term ozone exposure in China over 2013–2017. Environ. Int. 144, 106030 https://doi.org/10.1016/j.envint.2020.106030.

Westervelt, D.M., Ma, C.T., He, M.Z., Fiore, A.M., Kinney, P.L., Kioumourtzoglou, M.-A., Wang, S., Xing, J., Ding, D., Correa, G., 2019. Mid-21st century ozone air quality and health burden in China under emissions scenarios and climate change. Environ. Res. Lett. 14, 074030 https://doi.org/10.1088/1748-9326/ab260b.

Wu, K., Kang, P., Wang, Z., Gu, S., Tie, X., Zhang, Y., Wen, X., Wang, S., Chen, Y., Wang, Y., Chen, D., 2017. Ozone temporal variation and its meteorological factors over Chengdu city. Acta Sci. Circumst. 37, 4241–4252.

Wu, K., Yang, X., Chen, D., Gu, S., Lu, Y., Jiang, Q., Wang, K., Ou, Y., Qian, Y., Shao, P., Lu, S., 2020. Estimation of biogenic VOC emissions and their corresponding impact on ozone and secondary organic aerosol formation in China. Atmos. Res. 231, 104656 https://doi.org/10.1016/j.atmosres.2019.104656.

Wu, K., Wang, Y., Qiao, Y., Liu, Y., Wang, S., Yang, X., Wang, H., Lu, Y., Zhang, X., Lei, Y., 2022. Drivers of 2013–2020 ozone trends in the Sichuan Basin, China: impacts of meteorology and precursor emission changes. Environ. Pollut. 300, 118914 https://doi.org/10.1016/j.envpol.2022.118914.

Xie, M., Zhu, K., Wang, T., Yang, H., Zhuang, B., Li, S., Li, M., Zhu, X., Ouyang, Y., 2014. Application of photochemical indicators to evaluate ozone nonlinear chemistry and pollution control countermeasure in China. Atmos. Environ. 99, 466–473. https://doi.org/10.1016/j.atmosenv.2014.10.013.

Xie, M., Zhan, C., Zhan, Y., Shi, J., Luo, Y., Zhang, M., Liu, Q., Shen, F., 2021. Spatiotemporal variability of air stagnation and its relation to summertime ozone in the yangtze river delta of China. Front. Environ. Sci. 9, 783524 https://doi.org/10.3389/fenvs.2021.783524.

Xu, C., Chen, J., Li, Y., He, M., Feng, X., Han, L., Liu, Z., Qian, J., 2020. Emission inventory and characteristics of anthropogenic air pollution sources based on second pollution source census data in Sichuan Province[J]. Environ. Sci. 41 (10), 4482–4494.

Yang, J., Shao, M., 2021. Impacts of extreme air pollution meteorology on air quality in China. J. Geophys. Res. Atmos. 126 https://doi.org/10.1029/2020JD033210.

Yang, X., Wu, K., Wang, H., Liu, Y., Gu, S., Lu, Y., Zhang, X., Hu, Y., Ou, Y., Wang, S., Wang, Z., 2020. Summertime ozone pollution in Sichuan Basin, China: Meteorological conditions, sources and process analysis. Atmos. Environ. 226, 117392 https://doi.org/10.1016/j.atmosenv.2020.117392.

Yang, X., Wu, K., Lu, Y., Wang, S., Qiao, Y., Zhang, X., Wang, Y., Wang, H., Liu, Z., Liu, Y., Lei, Y., 2021a. Origin of regional springtime ozone episodes in the Sichuan Basin, China: role of synoptic forcing and regional transport. Environ. Pollut. 278, 116845 https://doi.org/10.1016/j.envpol.2021.116845.

Yang, X., Lu, Y., Wang, Y., Qiao, Y., Zhang, G., Wang, S., Zhang, X., Liu, Z., Liu, Y., Zhu, X., 2021b. Impact of synoptic patterns on regional ozone pollution in Sichuan Basin. China Environ. Sci. 41, 2526–2539.

Zhan, C., Xie, M., 2022. Land use and anthropogenic heat modulate ozone by meteorology: a perspective from the Yangtze River Delta region. Atmos. Chem. Phys. 22, 1351–1371. https://doi.org/10.5194/acp-22-1351-2022.

Zhao, K., Bao, Y., Huang, J., Wu, Y., Moshary, F., Arend, M., Wang, Y., Lee, X., 2019. A high-resolution modeling study of a heat wave-driven ozone exceedance event in New York City and surrounding regions. Atmos. Environ. 199, 368–379. https://doi.org/10.1016/j.atmosenv.2018.10.059.

Zheng, B., Tong, D., Li, M., Liu, F., Hong, C., Geng, G., Li, H., Li, X., Peng, L., Qi, J., Yan, L., Zhang, Y., Zhao, H., Zheng, Y., He, K., Zhang, Q., 2018. Trends in China's anthropogenic emissions since 2010 as the consequence of clean air actions. Atmos. Chem. Phys. 18, 14095–14111. https://doi.org/10.5194/acp-18-14095-2018.

Zheng, B., Zhang, Q., Geng, G., Chen, C., Shi, Q., Cui, M., Lei, Y., He, K., 2021. Changes in China's anthropogenic emissions and air quality during the COVID-19 pandemic in 2020. Earth Syst. Sci. Data 13, 2895–2907. https://doi.org/10.5194/essd-13-2895-2021.

Zhou, Z., Tan, Q., Deng, Y., Wu, K., Yang, X., Zhou, X., 2019. Emission inventory of anthropogenic air pollutant sources and characteristics of VOCs species in Sichuan Province, China. J. Atmos. Chem. 76, 21–58. https://doi.org/10.1007/s10874-019-9386-7.

Zhu, L., Mickley, L.J., Jacob, D.J., Marais, E.A., Sheng, J., Hu, L., Abad, G.G., Chance, K., 2017. Long-term (2005-2014) trends in formaldehyde (HCHO) columns across North America as seen by the OMI satellite instrument: evidence of changing emissions of volatile organic compounds: HCHO Trend across North America. Geophys. Res. Lett. 44, 7079–7086. https://doi.org/10.1002/2017GL073859.